ELSEVIER

Significance of kinetic theories on the recrystallization of kaolinite

K. Traoré [a], F. Gridi-Bennadji [b], P. Blanchart [b],*

[a] *Laboratoire de Physico-Chimie et de Technologie des Matériaux (LPCTM), Ouagadougou University,*
BP 7021, Ouagadougou 03, Burkina Faso
[b] *Ecole Nationale Supérieure de Céramique Industrielle (ENSCI), Limoges, France*

Abstract

Mathematical methods have been extensively used for the analysis of data obtained from non-isothermal thermal analysis of kaolinite or other clay minerals and Kissinger description is frequently considered. It is based on an Avrami-type transformation and an Arrhenian dependence of the reaction rate. In general, the calculation of the activation energy uses an incorrect neglect of the temperature dependence of the transformation rate. For kaolinite, Kissinger method applied to dehydroxylation gives an activation energy close to the measured enthalpy change for the reaction, but for recrystallization the activation energy exceeds the enthalpy change by a factor as high as 30. It is related to the complex character of recrystallization, since nucleation and crystal growth simultaneously occur, with the existence of both spinel and mullite phases. Consequently, the temperature dependence of recrystallization cannot be assumed to be Arrhenian. An interpretation is also found with Polanyi–Wigner equation applied to kaolinite transformations. Using thermodynamic data of entropy variation, the recrystallization rate should attain very high values, ranging from 5 to 10 order of magnitude over standard values for solid transformations. These observations cast some doubts on calculated activation energy of kaolinite recrystallization obtained from Kissinger kinetic method.
© 2006 Elsevier B.V. All rights reserved.

Keywords: DSC; Kissinger; Kaolinite

1. Introduction

Kaolinite is commonly used in sintered ceramic compositions. Differential scanning calorimetry (DSC) show a specific endothermic transformation at 823–973 K, due to the loss of structural hydroxyl groups and an exothermic peak at about 1253 K, due to the structural reorganization. The exothermal peak is generally interpreted with many controversial models, but the most accepted one describes the existence of either Al–Si spinel (similar to γ-alumina with variable content of Si) or mullite, depending on the nature of the precursor [1,2]. The reaction path, which gives orthorhombic mullite from metakaolinite, is explained by possible simultaneous reactions:

Metakaolinite (1253 K) → either:

(1) low crystallized alumino-silicate or spinel phase → (>1323 K) mullite;

(2) mullite with variable Al/Si ratio;
(3) amorphous silica → (>1253 K) cristobalite.

Silica is simultaneously crystallized and is involved in (1) and (2) reaction paths.

At higher temperature, up to 1323 K, increased amount of mullite is crystallized. A sequential phase formation was evidenced [1,3] with the co-existence of silica and an alumino-silicate phase. Nevertheless, attempts to determine the precise structural and chemical characteristics of phases [3] formed below 1273 K go against the accuracy of experiments and results are uncertain.

By X-ray diffraction, the respective quantity of Si–Al spinel and mullite formed at 1253–1873 K temperature was determined by Chakravorty [4], using a quantitative XRD technique. He estimated a high amount of spinel phase at 1253 K, i.e. 25–35 wt%, but no precise indications were reported about the thermal cycle (time interval at 1253 K) and no X-ray patterns are presented to validate results. Besides, mullite quantity below 1273 K was estimated at a very low level, which increases significantly above 1323 K. More recently, Chen et al. [2] presented XRD pattern

---

* Corresponding author. Fax: +33 555790998.
E-mail address: p_blanchart@ensci.fr (P. Blanchart).

of kaolin fired at 1273 K during 24 h. Whereas the very long stay at this temperature, only a wide and tenuous peak of spinel phase is seen, indicating the low amount of spinel with a high inaccuracy in its determination.

DSC curves of kaolinite and other clay minerals, present baseline instability and drift or uncertainty of peak limits, which interfere with measurements. Further experimental inaccuracies appear with the exothermal phenomenon because it occurs at high temperature (~1253 K) in a narrow temperature range and the transformation rate is very high. Consequently, isothermal methods cannot be effectively experimented and kinetic methods, as the Kissinger method, have been extensively used. Their common feature is the peak temperature measurement against the heating rate of DSC scans. For the interpretation of data, they use specific mathematical treatments with some assumptions for the calculations [5].

This paper presents an interpretation of DSC experiments of kaolinite, in temperature ranges of endothermic and exothermic phenomena. The significance of activation energy values calculated with Kissinger theory from DSC results is examined in comparison to calorimetric data relative to possible transformations. A comparison is also made with calculated thermodynamic data. The purpose is to assess the significance of the calculated activation energy of the kaolinite structural reorganization, obtained with the non-isothermal Kissinger method.

2. Theoretical background

The Jonhson–Mehl–Avrami equation is the most important theoretical basis. It describes the evolution with time t of the volume fraction crystallized x with the nucleation frequency I_v and the crystal growth rate u. Initially, it was used up to described glass crystallization, but was also applied to many material transformations. When I_v and u are supposed to be independent of time, the integral form is

$$x = 1 - \exp(-g' I_v u^{n-1} t^n) \tag{1}$$

where g' is a geometrical factor related to the growing phase and n is an integer which depends on crystallization mechanisms. In the case of an isothermal crystallization equation (1) becomes

$$x = 1 - \exp[(kt)^n] \tag{2}$$

k is defined as the overall reaction rate. It is assumed that k has an Arrhenian dependence with temperature:

$$k = k_0 \exp\left(\frac{E_a}{RT}\right) \tag{3}$$

where E_a is the apparent activation energy and k_0 is the frequency factor of the global crystallization process.

Eqs. (2) and (3) are the basis of crystallization interpretation in DSC experiments. It applies mainly to isothermal measurements, where all assumed conditions for theoretical treatments are completed. Nevertheless, they are also used to obtain expressions for the description of non-isothermal treatments and some authors proposed specific methods for analyzing thermo analytical data. The reaction rate dx/dt is obtained by taking the

differentiation of Eq. (2) with respect to time. This first step is employed in many approaches, as that proposed by Kissinger:

$$\frac{dx}{dt} = nk(1 - x)[-\ln(1 - x)]^{(n-1)/n} \tag{4}$$

In such expression, the parametric dependence of the reaction rate on temperature can be separated from its dependence on x. In this way, any subsequent operation as differentiation will be simplified

$$\frac{dx}{dt} = h(T)f(x) \tag{5}$$

There are number of possible formulation of $h(T)$ and $f(x)$, since both T and x are function of time. Different methods of analyzing DSC experiments results from different definitions of $h(T)$ and $f(x)$ and possible forms are reported in the literature [5]. In the case of Kissinger approach, the predominance of a first-order reaction where $f(x) = 1 - x$ and $n = 1$ was supposed.

Another assumption is made in the derivation of Eq. (4), where the quantity $A = [-\ln(1 - x)]^{(n-1)/n}$ is approximated as a constant value in a large range of x (0.25–0.75). This assumption is valid in the case of glass or gel recrystallization, because at the peak temperature the transformed fraction is approximately 0.5. For kaolinite in the peak region, the A quantity cannot be obtained accurately because the occurrence of complex and controversial reactions.

Kinetic theories are based on the comparison of DSC and DTG curves. It supposed that the maximum crystallization rate is at the DSC peak temperature, where the second derivative of x on t is zero. Derivation of Eq. (4) where $A =$ const. and taking k from Eq. (3) gives

$$\frac{d^2x}{dt^2} = Ak_0 \left(\frac{E}{RT_p^2} - \frac{Ak_0}{\beta} \exp\left(-\frac{E_a}{RT_p}\right) \right)$$
$$\times \beta(1 - x_p) \exp\left(-\frac{E_a}{RT_p}\right) \tag{6}$$

where β is the heating rate and x_p and T_p are the transformed fraction and temperature at the DSC peak.

When Eq. (6) is set to 0, it can be rewritten as

$$\frac{d \ln[\beta/T_p^2]}{d(1/T_p)} = -\frac{E_a}{R} \tag{7}$$

A plot of $\ln[\beta/T_p^2]$ against $1/T_p$, should gives a straight line, which slope is E_a/R.

The Kissinger method provides a single activation energy, which is commonly interpreted as an energy barrier. But kaolinite transformation involves a sequence of elementary phenomena as phase nucleation and growth with different energy barriers. Refined methods for obtaining the distribution of energy barrier are proposed, as the differential isoconversional method of Friedman [6] or the more recent integral isoconversional method of Vyazovkin and Dranca [7]. The applicability of these methods to kaolinite structural reorganization is strongly related to the validity of experimental data. Particularly the exact shape of peaks must be accurately obtained.

Table 1
Kaolin composition

Chemical (mass%)		Mineralogical
SiO_2	44.2	Kaolinite $= 96 \pm 2$
Al_2O_3	39.6	
Fe_2O_3	0.2	Quartz $< 1 \pm 0.2$
TiO_2	1.4	
MgO	0.03	
Na_2O	0.01	Anatase $> 1 \pm 0.2$
K_2O	0.05	
P_2O_5	0.03	Gibbsite $> 2 \pm 0.3$
Loss at 1273 K	13.78	
Others	0.7	

Fig. 1. DSC of kga-1b at different heating rates.

Fig. 2. Kissinger plot for the exothermal peak in the 1243–1293 K temperature range.

3. Experimental

The kaolinite used is the very high purity and reference material kga-1b from the Clay Mineral Society (University of Missouri, USA). This raw material is well-known and present very reproducible chemical [8,9] and mineralogical compositions, which are listed in Table 1. Before characterizations, the material was grounded, sieved below 40 μm and dried at 373 K, during 2 h.

Differential scanning calorimetry was performed using a Setsys 2400 apparatus from SETARAM equipped with a DSC 1500 head system with Pt crucibles. For kinetic interpretations, the instrument was used in the temperature-scanning mode and all experiments were performed from room temperature to 1573 K using six different heating rates (3, 5, 8, 10, 15 and 20 K min^{-1}). Each experiment was carried out with 100 mg of compacted powder into the crucible and a pure α alumina powder heated at 1773 K serves as reference material in adequate quantity to reduce the calorimeter imbalance. The kiln atmosphere was air under ambient atmospheric pressure.

Calorimetric methods were conducted to measure the transformation heat during both endothermic and exothermal phenomena. Since the area under a peak is proportional to heat released (ΔQ), an accurate calibration was performed using phase transformations: –$SrCO_3$ at 1197 K (Aldrich; purity 99.995%); –K_2SO_4 at 857 K (Aldrich; purity 99.99%). In addition, calibrations were performed at the six heating rates used. Specific care was taken to avoid small inaccuracy from the baseline position, which can be drifted by thermal imbalances [10]. From results of preliminary calibrations, we corrected all curves by subtracting a linear function between the onset and the end of peaks. ΔQ is determined by integrating dQ/dt versus t.

Kaolinite materials were also characterized after different thermal cycles and quenching. Powder X-ray diffraction was performed using a step scan of $0.02°\ 2\theta$ and 13 s per step (Brüker AXS, D5000 diffractometer, Cu Kα radiation source, graphite back-monochromator). To avoid any preferential orientation, all grounded sample were loaded in a side-drifted way, into a grooved sample holder. Transmission microscopy (TEM) equipment was a JEOL2010 (100 kV) and samples were preliminary thinned and ion-etched under Ar.
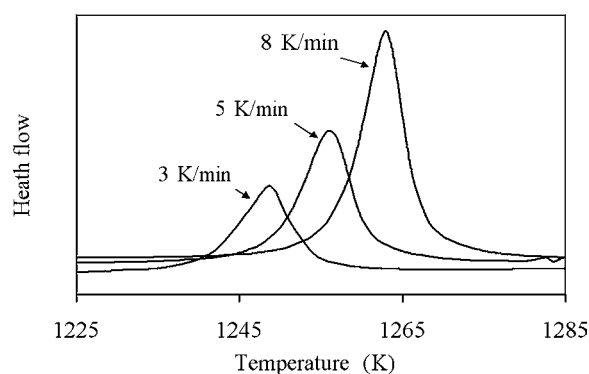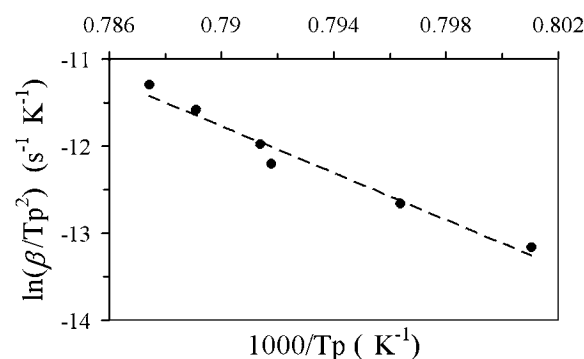
4. Results

Fig. 1 presents three typical DSC curves of kga-1b in the temperature interval of the exothermal phenomenon. The shift of peak position against the heating rate is significant and the peak temperature can be determined with precision. For the 6 heating rates used, the Kissinger plot (Eq. (7)) can be fitted with a straight line (Fig. 2) and the calculated activation energy is 1123 ± 60 kJ mol^{-1}. From peak surfaces, ΔQ values are reported in Table 2 for the endothermic and exothermal phenomena. They weakly vary with the heating rate that ensures the validity of the experimental method used. Since ΔQ is obtained at constant atmosphere pressure and composition, in a similar temperature range, the equality $\Delta Q = \Delta H$ is assumed.

Experimental ΔH can be compared to calculated one from tabulated thermodynamic data [11]. In the case of ideal transformations of an alumino-di-silicate in alumina or mullite and

Table 2
Enthalpy variations from calorimetric measurements for dehydroxylation and structural reorganization

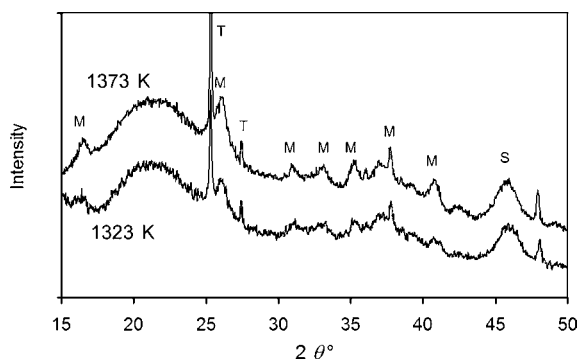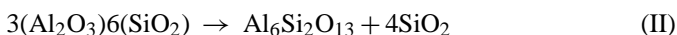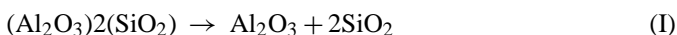| Heating rate (K min^{-1})	ΔQ_{endo} (kJ mol^{-1})	ΔQ_{exo} (kJ mol^{-1})
20	194	−36
10	200	−35
5	202	−30
3	207	−31

Fig. 3. X-ray patterns for kga-1b at 1323 and 1373 K (10 K min^{-1}, 2 h). M: mullite; T: TiO$_2$; S: Al–Si spinel.

silica:

$$(Al_2O_3)2(SiO_2) \rightarrow Al_2O_3 + 2SiO_2 \qquad (I)$$

$$3(Al_2O_3)6(SiO_2) \rightarrow Al_6Si_2O_{13} + 4SiO_2 \qquad (II)$$

Values of $\Delta H = 280$ kJ mol^{-1} for reaction (I) and $\Delta H = 810$ kJ mol^{-1} for reaction (II) are obtained.

Thermodynamic data can be correlated to structural information from X-ray patterns of kga-1b at temperature above the exothermic peak. Both 1323 and 1373 K patterns show broad reflections of mullite and Al–Si spinel whereas TiO$_2$ from the initial kaolin is identified. When the temperature increases, spinel reflection are not changed, but mullite peaks increase in size (Fig. 3).

5. Discussion

Kissinger theory applied to kaolinite dehydroxylation gives apparent activation energies from 140 to 210 kJ mol^{-1} [12–16] and 23 kJ mol^{-1} in a more recent publication [17]. Obtained values are strongly related to the kaolinite type and the atmosphere pressure during heating. Literature data are equivalent to our experimental results (209 kJ mol^{-1}) and are comparable to data from the calorimetric method (194–207 kJ mol^{-1} in Table 2). The small decrease of data with the increase of the heating rate is related to the change of involved mechanisms. Since dehydroxylation is related to the breaking of chemical bonds and to chemical diffusion within the phyllosilicate structure, a higher heating rate favors the water diffusion process outside particles [18].

For the exothermal peak at about 1253 K, the apparent activation energy from kinetic methods is strongly related to amount and type of kaolinite and associated minerals. The atmosphere during heating and the thermal history of kaolinite are also influent parameters. Published data are in the range 500–1150 kJ mol^{-1}, but they vary strongly with the structural characteristics of the high temperature form of kaolinite (metakaolinite) and with the thermal process [1,2]. The reaction path, which follows either reaction (I) or (II) depends in the kaolinite type and processing methods [19]. In general, spinel and mullite occurs simultaneously below 1373 K, but no strict relationship was found between the kaolinite type and the experimental values of ΔH or E_a. Particularly, E_a also depends on the kinetic model used and on the fundamental understanding of the mathematical treatment of data.

The controversial E_a value point to the validity of the analytical method proposed by Kissinger, which is based on the mathematical transformation of Eq. (1). But in manipulating the basic expressions, Kissinger made some assumptions, which are far from the physical aspect of crystallization mechanisms in kaolinite.

The supposition of an Arrhenian dependence of k with temperature in Eq. (2) should hold when both the crystal growth and the nucleation frequency have Arrhenian dependence with temperature. This situation was observed with many glasses, which exhibit a separation between curves of nucleation and crystal growth rates as a function of temperature [20]. However, when more complex mechanisms occur simultaneously, as surface and bulk crystallization, the overall crystallization process is governed by the heating rate and the Arrhenius relation is no longer valid. It is the case with kaolinite which undergone a complex structural reorganization process. X-ray results of kga-1b at 1323 and 1373 K (Fig. 3) show the occurrence of both broad spinel and mullite peaks at 1323 K (10 K min^{-1}, 2 h), whereas small mullite peaks increase in size at 1373 K and small spinel peaks can be distinguished. For the same material, a TEM observation (Fig. 4) after heating at 1323 K (5 K min^{-1}) during 4 h clearly shows nano-crystallites of mullite, which number density is small. When the thermal cycle change (1373 K, 10 K min^{-1}), both mullite size and number density of crystallite are clearly changed (Fig. 5). Consequently, results of materials heated below 1273 K support the very low quantity of crystallized spinel and mullite. When materials are heated above 1273 K we observe the continuous nucleation and growth of mullite and the progressive disappearance of spinel phase. It means a large overlap of nucleation and crystal growth processes for both phases and a strong temperature dependence.
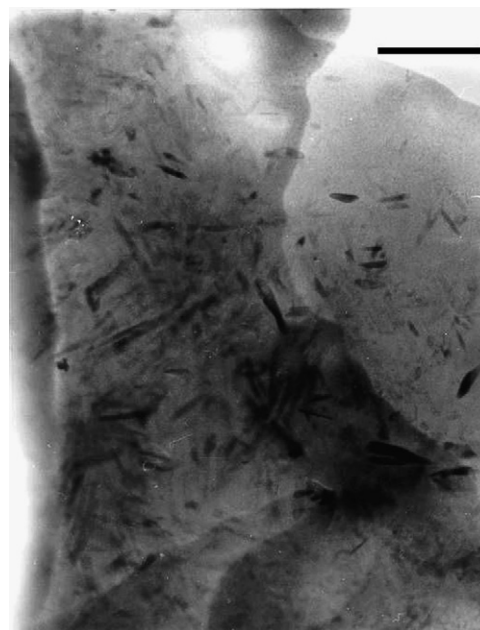

Fig. 4. TEM photo of kga-1b after heating at 1323 K (5 K min^{-1}, 4 h). Nano-crystallites of mullite are in dark grey. Bar = 20 nm.
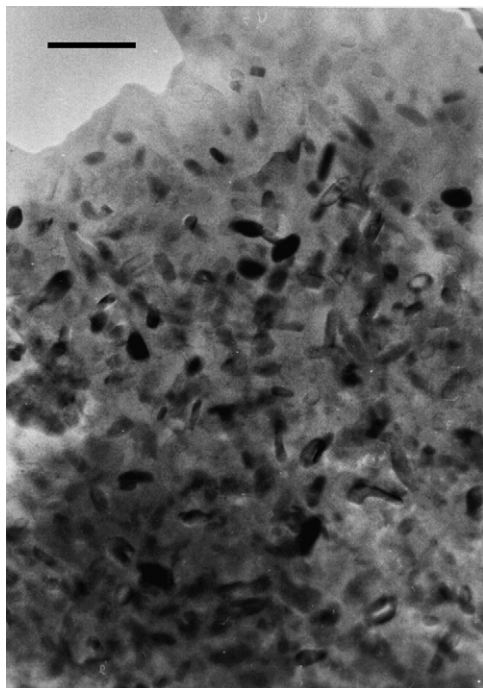
Fig. 5. TEM photo of kga-1b after heating at 1373 K (10 K min^{-1}, 4 h). Bar = 20 nm.

A similar observation was made in the literature, where the nucleation frequency of phase in kaolinite was described as a non-Arrhenian mechanism [21].

An explanation is found with the heterogeneous character of metakaolinite at a small scale [22]. Besides homogeneous mechanisms, interface-controlled mechanism also occurs, indicating a strong temperature dependence. In addition, the crystal growth rate was described with only some data [19], which significance depends in the obvious overlapping of nucleation and growth phenomena. Consequently we cannot neglect the complicate dependence of nucleation frequency with temperature and the reaction rate k cannot be approximated as an Arrhenian over a temperature range near the peak temperature.

An alternative approach to the theoretical basis of Arrhenius is proposed with the Polanyi and Wigner description. Arrhenius approach is well established for homogenous rate processes, but in solid materials this model is questioned, because the existence of local variations of activation energy. Nevertheless, in heterogeneous materials, energy is rapidly transferred between constituents and an average energy must be considered. In that case, Polanyi and Wigner proposed a theoretical description of an activated reaction occurring at an advancing interface [23]. The thermodynamic basis of the activation process in the case of an irreversible reaction is written under the form:

$$\frac{\mathrm{d}x}{\mathrm{d}t} = \left(\frac{k_{\mathrm{B}} T}{h} \right) x_0 \exp\left(-\frac{\Delta H}{RT} \right) \exp\left(\frac{\Delta S}{R} \right) \qquad (8)$$

where k_{B} and h are Boltzmann and Planck constants.

This equation relates enthalpy and entropy variations to the frequency factor k_0 and to the activation energy through Eqs. (3) and (4). Polanyi and Wigner equation can be used to estimate values of entropy variation and frequency factor, when enthalpy changes during transformations are known.

In the case of the endothermic transformation, Eq. (8) can be applied using ΔH reported in Table 2 and E_{a} from the literature. Calculated frequency factor $k_0 \sim 10^{15}$ S^{-1} and entropy variation $\Delta S = -50$ J K mol^{-1} are similar to published data [24].

For the exothermal transformation, calculated E_{a} (500–1150 kJ mol^{-1}) exceed ΔH (Table 2) by a factor of 30. If we ascribe a nominal value of $k_0 = 10$ [21,22] in the Polanyi and Wigner equation [1,25], we found that the entropy variation exceed reasonable values, as high as $\Delta S = -700$ J K^{-1} mol^{-1}. This value must be compared to that calculated from thermodynamic data, in the case of alumino-di-silicate transformation to either alumina or mullite and silica. $\Delta S = -16$ J K^{-1} mol^{-1} for reaction (I) and $\Delta S = -22$ J K^{-1} mol^{-1} for reaction (II) are obtained. They are very different from calculated ΔS in the Polanyi and Wigner equation, which further cast some doubt on the activation energy data obtained from kinetic methods applied to the exothermal phenomenon of kaolinite.

6. Conclusion

With kaolinite in the 1223–1293 K temperature range, nucleation and crystal growth processes occur simultaneously. XRD and microscopy experiments clearly show the simultaneous existence of spinel and mullite phases from a non-homogeneous process. With kaolinite, the temperature dependence of the reaction rate cannot be assumed to be Arrhenian.

Even though kinetic methods can be used to characterize the exothermal transformation at 1253 K, the activation energy is found to exceed widely the overall enthalpy change of the reaction. Since the entropy variation of the reaction is known, the transformation rate calculated with Polanyi and Wigner equation attain a very high value, which exceed significantly literature data of transformation rate. Besides, TEM observations evidence the existence of a slow crystallization process. We conclude that the Kissinger approach is not an appropriate method for the interpretation of kaolinite transformation at 1253 K. A suitable theoretical interpretation could be proposed when the exact nature of phenomenon involved in the exothermal transformation will be identified.

References

[1] A. Gualtieri, M. Bellotto, G. Artioli, S.M. Dark, Phys. Chem. Miner. 22 (1995) 215–222.
[2] Y.-F. Chen, M.-C. Wang, M.-H. Hon, J. Eur. Ceram. Soc. 24 (2004) 2389–2397.
[3] S. Lee, Y.J. Kim, H.-S. Moon, J. Am. Cearm Soc. 82 (1999) 2841–2848.
[4] A.K. Chakravorty, D.K. Ghosh, J. Am. Ceram. Soc. 74 (1991) 1401–1406.
[5] E. Brown, Handbook of Thermal Analysis and Calorimetry, Elsevier, Amsterdam, 1998.
[6] H. Friedman, J. Polym. Sci. 6 (1964–1965) 183–189.
[7] S. Vyazovkin, I. Dranca, Macromol. Chem. Phys. 207 (2006) 20–25.
[8] R.J. Pruett, H.L. Webb, Clays Clay Miner. 41 (1993) 514–549.
[9] E. Papirer, A. Eckhardt, F. Muller, J. Yvon, J. Mater. Sci. 25 (1990) 5109–5117.

[10] M.J. Starink, P.J. Gregson, Scrip. Metall. Mater. 33 (1995) 893–900.

[11] G.W. Samsonov, The Oxide Handbook, 2nd ed., IFI/Plenum, New York, 1982.

[12] G.W. Brindley, J.H. Sharp, J.H. Patterson, B.N. Narahari Achar, Am. Miner. 52 (1967) 201–211.

[13] I. Horvath, Thermochim. Acta 85 (1985) 193–198.

[14] S.A.T. Redfern, Clay Miner. 22 (1987) 447–456.

[15] M. Bellotto, A. Gualtieru, G. Artioli, S.M. Dark, Phys. Chem. Miner. 22 (1995) 207–214.

[16] P. Dion, J.F. Alcover, F. Bergaya, A. Ortega, P.L. Llewellyn, F. Rouquerol, Clay Miner. 33 (1998) 269–276.

[17] K. Nahdi, P. Llewellyn, F. Rouquérol, J. Rouquérol, N.K. Ariguib, M.T. Ayedi, Thermochim. Acta 390 (2002) 123–132.

[18] M. Bellotto, A. Gualtiery, G. Artioli, S.M. Dark, Phys. Chem. Miner. 22 (1995) 207–214.

[19] O. Castelein, B. Soulestin, J.P. Bonnet, P. Blanchart, Ceram. Int. 27 (2001) 517–522.

[20] X. Guo, H. Yang, M. Cao, J. Non-Cryst. Solids 351 (2005) 2133–2137.

[21] V.M. Fokin, M.L.F. Nascimento, E.D. Zanotto, J. Non-Cryst. Solids 351 (2005) 789–794.

[22] F. Bergaya, P. Dion, J.F. Alcover, C. Clinard, D. Tchoubar, J. Mater. Sci. 31 (1996) 5069–5075.

[23] D.A. Young, Decomposition of Solids, Pergamon, 1966.

[24] I. Horvath, React. Solids (Amsterdam) 7 (1989) 173–181.

[25] M. Romero, J. Martin-Marquez, J.Ma. Rincon, J. Eur. Ceram. 26 (2006) 1647–1652.